

## The crystal structure of hutchinsonite, $(\text{Tl,Pb})_2\text{As}_5\text{S}_9$

By Y. TAKÉUCHI\*, SUBRATA GHOSE\*\* and W. NOWACKI

Abteilung für Kristallographie und Strukturlehre, Mineralogisches Institut,  
Universität Bern (Schweiz)<sup>1</sup>

With 14 figures

(Received November 14, 1964)

### Auszug

Die vollständige Kristallstruktur von Hutchinsonit wurde bestimmt. Die neuen chemischen Analysen des Minerals zeigen, daß Ag und Cu keine wesentlichen Bestandteile sind. Sie ergeben eine Idealformel  $(\text{Tl,Pb})_2\text{As}_5\text{S}_9$  statt wie früher angegeben  $(\text{Tl,Pb})_2(\text{Ag,Cu})\text{As}_5\text{S}_{10}$ . Die Raumgruppe ist  $D_{2h}^{15}\text{-Pbca}$  und die Gitterkonstanten sind  $a = 10,81 \pm 0,01 \text{ \AA}$ ,  $b = 35,36 \pm 0,04 \text{ \AA}$  und  $c = 8,16 \pm 0,01 \text{ \AA}$  mit 8 Formeleinheiten pro Zelle. Die direkte Interpretation der dreidimensionalen Patterson-Funktion lieferte durch Anwendung geometrischer Beziehungen zwischen „cross vectors“ für die gegebene Raumgruppe die Lage der schweren Atome. Sukzessive dreidimensionale Fourier-Synthesen ergaben die Orte der anderen Atome. Die Strukturverfeinerung wurde mittels Differenz-Fourier-Synthesen und schließlich mittels dreidimensionaler Least-square-Methoden vorgenommen.

Die erhaltene Struktur bestätigt die neue chemische Formel. Die Struktur besteht aus zwei Arten von Schichtpaketen parallel (010). In dem einen befinden sich parallel  $c$   $\text{As}_4\text{S}_8$ -Spiralen, welche — seitlich durch andere  $\text{AsS}_3$ -Pyramiden miteinander verbunden — eine komplexe Schicht parallel (010) bilden. Im anderen treten endliche  $\text{As}_2\text{S}_5$ -Gruppen auf. Die  $c$ -Projektion dieses Paketes ähnelt einem verzerrten  $\text{PbS}$ -Gittertyp. Die Tl- und Pb-Atome sind von sieben Schwefelatomen koordiniert. Die gefundene Struktur gibt eine Erklärung für die gute Spaltbarkeit parallel (010).

### Abstract

The crystal structure of hutchinsonite has been determined. The new chemical analyses of the mineral showed that Ag and Cu are not essential components, and give an ideal formula  $(\text{Tl,Pb})_2\text{As}_5\text{S}_9$  instead of previously assigned

<sup>1</sup> Contribution no. 150. Part 17 of papers on sulfides.

\* Present address: Mineralogical Institute, University of Tokyo, Tokyo, Japan.

\*\* Present address: Institut für Kristallographie und Petrographie, E.T.H., Zürich, Schweiz.

(Tl, Pb)<sub>2</sub>(Ag, Cu)As<sub>5</sub>S<sub>10</sub>. The space group is  $D_{2h}^{15}-Pbca$ , and the lattice constants are  $a = 10.81 \pm 0.01 \text{ \AA}$ ,  $b = 35.36 \pm 0.04 \text{ \AA}$ ,  $c = 8.16 \pm 0.01 \text{ \AA}$ . There are 8 formula units in the cell. Using geometrical relationships among cross vectors for the space group under consideration, a direct interpretation of the three-dimensional Patterson function yielded the locations of the heavy atoms. Locations of other atoms were found by successive three-dimensional Fourier syntheses. The refinement of the structure was performed by difference-Fourier trials, and finally by the three-dimensional least-squares method.

The structure obtained confirms the new chemical formula. The bulk of the structure consists of two kinds of slabs, both running parallel to (010). In one kind of slab, there are As<sub>4</sub>S<sub>8</sub> spiral chains along the *c* axis. These chains are joined together laterally by other AsS<sub>3</sub> pyramids, forming a complex layer parallel to (010). In the other, As—S groups form a finite group As<sub>2</sub>S<sub>5</sub>. The *c* axis projection of this slab resembles a distorted PbS-type structure. The Tl and Pb atoms are coordinated by seven sulfur atoms. The proposed structure explains well the good cleavage parallel to (010).

### Introduction

Based upon the ratio As:Pb, the series of sulfosalts whose chemical formulae are approximately of the type  $x\text{Pb(Tl)S} \cdot y\text{As}_2\text{S}_3$  may be classified into three groups. Contained in the first group are jordanite, gratonite (RÖSCH, 1963) and lengenbachite. The As:Pb ratios of these minerals are in the range  $\sim 0.44 - \sim 0.67$ , and show a high content of Pb (cf. NOWACKI, 1964). The structures of these sulfosalts are characterized by marked PbS substructures. To the second group belong rathite, dufrenoyite (LEBIHAN, 1962; NOWACKI *et al.*, 1963a,b), baumhauerite (LEBIHAN, 1962; NOWACKI *et al.*, 1964) and scleroclase (NOWACKI *et al.*, 1961). For this group the ratio varies from 1.29 (rathite I) to 2.00 (scleroclase). The structures of these minerals are built up of layers which have the periodicities 8.4 Å (or a multiple of 4.2 Å) and 7.9 Å in the directions of two-dimensional extension. The ways of stacking these layers, and slight changes in the chemical composition of the layer, differentiate various structures.

The mineral hutchinsonite belongs to the final group, showing the highest ratio, 2.50. Hutchinsonite is thus the richest in arsenic among these sulfosalts, and x-ray photographs of this mineral show neither a PbS substructure nor evidence of the layer structure as in the minerals of the second group. Accordingly a different structural scheme than that found in other minerals of this series can be expected for hutchinsonite. The crystallographic description of the mineral has been presented by NUFFIELD (1947). A brief account of the present work has already appeared (TAKÉUCHI *et al.*, 1964).

### Experimental

Specimens used for the present investigation are those from Lengnabach in the Binnatal, Valais, Switzerland. Short, prismatic, single crystals were separated from dolomite, and good crystals were selected for x-ray investigation; the rest was used for the chemical analyses.

The lattice constants previously reported (TAKÉUCHI *et al.*, 1964) were re-examined by taking zero-level Weissenberg photographs on which calibration powder patterns of KCl were recorded. The unit-cell dimensions obtained for the orthorhombic cell are as follows:

$$a = 10.81 \pm 0.01 \text{ \AA}, \quad b = 35.36 \pm 0.04 \text{ \AA}, \quad c = 8.16 \pm 0.01 \text{ \AA}.$$

For the lattice constant of KCl the value 6.2931 Å (SWANSON and TATGE, 1953) was used. These values are in good agreement with those of NUFFIELD. The space group  $D_{2h}^{15} - Pbca$  assigned by NUFFIELD (1947) was confirmed. The observed conditions limiting reflections  $hk0$  with  $h = 2n$ ,  $h0l$  with  $l = 2n$  and  $0kl$  with  $k = 2n$  only, are unique for the space group  $D_{2h}^{15} - Pbca$ . There is no possibility of other space groups of lower symmetry unless some special arrangements of atoms are assumed.

A spherical specimen with radius 0.118 mm was prepared for the intensity determinations. The three-dimensional intensities were recorded on multiple films by an integrating Weissenberg camera, using  $CuK\alpha$  radiation, and they were measured with the help of a Joyce-Loebl microdensitometer. Intensities were corrected for Lorentz, polarization and absorption factors, using IITAKA's program written for the Bull-Gamma-A.E.T. computer.

### Chemical composition

Two chemical analyses have been reported for hutchinsonite from Binnatal (SMITH and PRIOR, 1907). In his crystallographic investigation, NUFFIELD suggested that the above chemical analyses lead to an ideal formula  $(Pb,Tl)_2(Ag,Cu)As_5S_{10}$  by assuming  $d = 5.18$ , in contrast to the observed value  $d = 4.6 \text{ g cm}^{-3}$  (SMITH and PRIOR, 1907). Although the assumption of the specific gravity made by NUFFIELD seems to be reasonable, our new chemical analyses show somewhat different results. The several analyses are compared in Table 1, from which it can be observed that the contents of Ag and Cu are exceedingly small in the new analyses. To confirm this, a spectroscopic analysis was performed by S. GRAESER using the fragments of

Table 1. *Chemical analyses of hutchinsonites*

	SMITH and PRIOR		New analysis		Ideal formula	
	1	2	3	4	I	II
Pb	12.5%	16%	18.92%	17.3%	17.06%	19.28%
Tl	25	18	21.03	20.0	16.83	19.02
Ag	9	2	ca. 0.11	—	8.88	
Cu	—	3	0.96	—		
Fe	—	0.5	—	—		
As	30.5	29.5	31.66	36.8	30.84	34.86
Sb	—	2	—	—		
S	26	26.5	27.32	26.5	26.39	26.84
Total	103.0	97.5	100.0	100.6	100.00	100.00

3. Ordinary microchemical analysis. Original analysis contains 4.63% H<sub>2</sub>O, < 105°C. The values in the table are normalized to 100% (Fresenius, Wiesbaden)

4. Electron-microprobe chemical analysis (NOWACKI and BAHEZRE, 1963).

I. (Tl,Pb)<sub>2</sub>AgAs<sub>5</sub>S<sub>10</sub>,  $d = 5.18$ .

II. (Tl,Pb)<sub>2</sub>As<sub>5</sub>S<sub>9</sub>,  $d = 4.58$ .

Table 2. *Number of atoms in the cell*

calculated from the results of four chemical analyses as given in Table 1

		Tl + Pb	Ag(+Cu)	As(+Sb)	S
$d = 5.18$	1	17.7	8.16	39.6	79.0
	2	16.0	6.4	40.0	80.4
	3	18.9	1.6	41.1	82.8
	4	18.1	—	47.8	80.4
$d = 4.6$	1	15.4	6.4	35.2	70.6
	2	14.6	5.8	36.24	73.2
	3	16.72	1.4	36.4	73.8
	4	15.7	—	42.2	71.0

the single crystals used for intensity determination. The result showed only traces of Cu, Ag and Zn in addition to the other main components.

The calculated numbers of atoms in the unit cell are compared in Table 2 for  $d = 5.18$  and  $d = 4.6$  g cm<sup>-3</sup>. Since it would be reasonable to assume that all the atoms are distributed over the general positions of the space group  $D_{2h}^{15} - Pbca$ , the number of atoms is expected to be a multiple of 8. It is seen in Table 2, that for  $d = 4.6$  the results of our new analyses give a unit-cell formula which is close to an ideal form, (Tl,Pb)<sub>16</sub>As<sub>40</sub>S<sub>72</sub>. If we adopt  $d = 5.18$ , our results show some deviation from the formula given by NUFFIELD, especially in the

number of Pb + Tl atoms. On the other hand, the results by SMITH and PRIOR show better agreement with the formula suggested by NUFFIELD for  $d = 5.18$ . Because of this ambiguity, it did not seem possible to draw a definite conclusion from these results. We therefore proceeded with the structure analysis, bearing both possibilities in mind. In either case, there are two Tl(Pb) atoms in the asymmetric unit. Accordingly, if the positions of these atoms could be found, it was expected it would be possible to determine the structure regardless of the ambiguity in the chemical formula.

### Structure analysis

#### *Preliminary*

The three-dimensional Patterson map  $P(uvw)$  was obtained from the  $F^2(hkl)$ 's. It was observed from the map that most of the heavy peaks are distributed on the sections  $z = 0$ ,  $\frac{1}{4}$  and  $\frac{1}{2}$ , suggesting that the  $z$  parameters of the heavy atoms are roughly  $\frac{1}{8}$  or  $\frac{3}{8}$ . Two sections,  $w = \frac{1}{4}$  and  $\frac{1}{2}$ , are shown in Fig. 1. Since the origin peak of the map has the weight 1800, the expected single weight in the map is  $\sim 80$  for Pb(Tl) — Pb(Tl),  $\sim 35$  for Pb(Tl) — As and  $\sim 15$  for Pb(Tl) — S. The Patterson map is also characterized by heavy peaks arranged nearly at the intersections of the net  $\frac{n}{16} \cdot b \times \frac{m}{4} \cdot a$ , where  $n$  and  $m$  are integers. As a matter of fact,  $F(0,16,0)$  and  $F(400)$  are outstandingly strong reflections. From geometrical relations among a symmetrical set of atoms for the space group  $D_{2h}^{15} - Pbca$  [Fig. 2(b)], the possible candidates for the  $c$ -screw satellites of the Pb(Tl) — Pb(Tl) symmetrical pairs were derived. They are indicated by  $S$ ,  $D$ ,  $E$  and  $H$  in Fig. 1. Since there should be only two  $c$ -screw satellites in a quarter of the cell, some of them must be spurious. Inversion peaks were derived from each satellite, and then finally eight possible combinations of two Pb(Tl) atoms were obtained. It should be noted that all these combinations give positive signs for  $F(0,16,0)$ ,  $\bar{U} = 0.41$ , and negative for  $F(400)$ ,  $\bar{U} = 0.55$ , suggesting that most of the heavy peaks are nearly in the shaded areas shown in Fig. 3. The  $\bar{U}$  values are the averages of those obtained from the two possible chemical compositions.

Among these combinations, only two are consistent with the vector map  $P(\frac{1}{2}vw)$ . They are listed in Table 3. These two possible sets of Pb (Tl) atoms may be used to find the correct structure by refining the structures which would be derived from each set. However, in view of

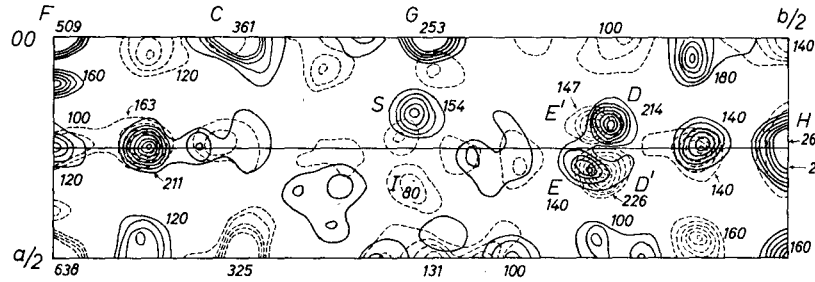


Fig. 1. Patterson sections,  $z = \frac{1}{2}$  and  $z = \frac{1}{4}$ , of hutchinsonite. Peaks in the section  $z = \frac{1}{2}$  are shown by solid contours and those in the section  $z = \frac{1}{4}$  by broken. Numbers indicate heights of peaks

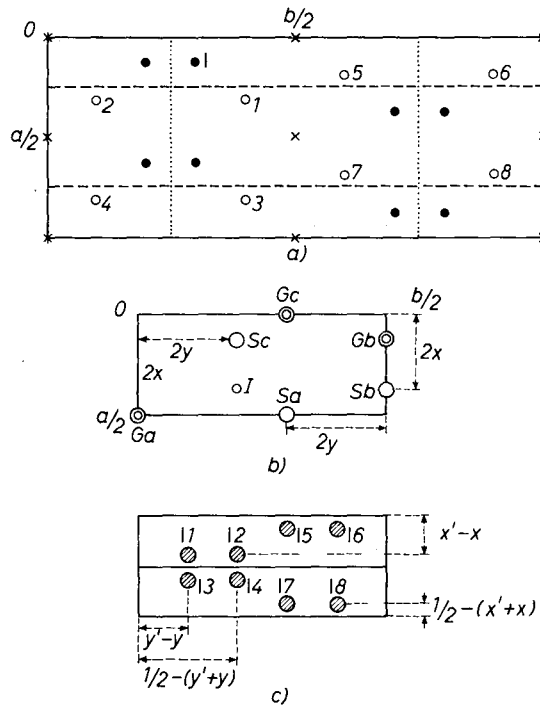


Fig. 2. (a) Two independent sets of atoms in the space group  $D_{2h}^{15}-Pbca$  (a glide and screw axes are not shown) (b) Geometrical relationship between an inversion peak, I, and its screw (single circle) and glide-reflection satellites (double circle) in the Patterson diagram having the symmetry  $D_{2h}^1-Pmmm$ . The example corresponds to the set of white atoms in (a). The  $z$  coordinates for each peak are:

I	Sa	Sb	Sc	Ga	Gb	Gc
$2z$	$2z$	$\frac{1}{2}-2z$	$\frac{1}{2}$	$\frac{1}{2}-2z$	$0$	$\frac{1}{2}$

(c) An example of peaks due to cross vectors between a set equivalent to the white atom  $x, y, z$  and a set equivalent to the black atom  $x', y', z'$ . The  $z$  coordinates are:

$$\begin{array}{l} \left| \begin{array}{l} 1 \text{ and } 6: z' - z, \\ 2 \text{ and } 5: \frac{1}{2} + (z' - z), \end{array} \right. \quad \left| \begin{array}{l} 3 \text{ and } 8: \frac{1}{2} - (z + z'), \\ 4 \text{ and } 7: z + z'. \end{array} \right. \end{array}$$

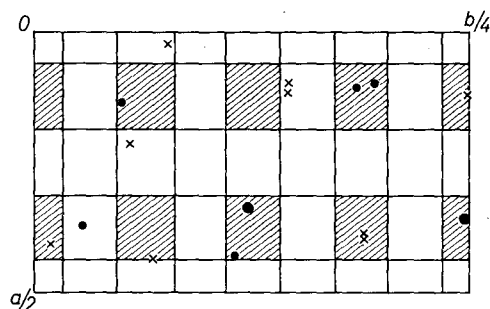


Fig. 3. Shaded area indicate common area for  $+F(0,16,0)$  and  $--F(4,0,0)$ . The final atomic positions are indicated. Big solid circle: Pb(Tl); small solid circle: As; cross: S

Table 3. Possible combination of (Tl, Pb) locations

Com- bination	Pb(Tl) <sub>I</sub>			Tl(Pb) <sub>II</sub>			Corresponding <i>c</i> -screw satellite
	<i>x</i>	<i>y</i>	<i>z</i>	<i>x</i>	<i>y</i>	<i>z</i>	
A	.1525	.1878	.125	.1525	.1878	.625	<i>D</i>
B	.37	.25	.125	.336	.123	.125	<i>S, H</i>

the difficulty encountered with the chemical composition, it was strongly desired to derive the structure by some straightforward means. It was then found that a unique solution of the Patterson function could be obtained if we applied the geometrical relationships among cross vectors — the vectors occurring between independent symmetrical sets of atoms.

#### *Use of cross vectors to find inversion peaks*

In Patterson space, some rules exist regarding the distribution of points due to cross vectors. For axial symmetries the relationships have been discussed in some detail by BUEGGER (1959, pp. 115). For glide planes, relationships among cross vectors may offer a possible criterion with which to select the correct inversion peaks. An example of the distribution of points due to cross vectors is given in Fig. 2(c) for the space group  $D_{2h}^{15} - Pbc_a$ . Since the space group has the *a* glide, in the *c*-axis projection, the Patterson map has a pseudotranslation  $a/2$ , giving rise to a mirror plane at  $\frac{1}{4}y$  of the actual unit cell. Although in three dimensions, the mirror plane is missing, for each point  $u, v, w$  due to a cross vector  $A - B$  occurring between independent sets of

atoms  $\{\mathbf{r}_A\}$  and  $\{\mathbf{r}_B\}$ , there is always a "pair point"  $\frac{1}{2} - u, v, w'$  due to a second vector  $A - B$ . This point has the same weight as that of the first, and it is related to the first by a mirror operation across the plane  $\frac{1}{4}, y, z$ , plus some component,  $w' - w$ , along the  $c$  axis. Although a similar geometrical relation exists between an inversion peak and its  $c$ -screw satellite peak, they have different weight, the weight of the latter being twice that of the former. So, even if the peaks due to cross vectors occur in the same plane or line where satellite peaks are expected, they can in principle be distinguished by searching their "pair peaks", i.e. peaks having the same weight at the locations indicated above. Similar relations can be observed for other sets of glide planes in  $D_{2h}^{15} - Pbca$ . However, consideration of the pair peaks due to one convenient set of glide planes, i.e. the glide planes perpendicular to the shortest axis, may generally offer conclusive results. A thorough investigation by listing all possible  $A - B$  vectors will not be necessary to find acceptable inversion peaks.

Table 4. Number of peaks due to  $Tl(Pb) - Tl(Pb)$  vectors

	Weight	Equivalent set I	Equivalent set II
Inversion	1	8	8
Screw satellite	2	12	12
Glide satellite	4	6	6
Cross vector	2		64

As seen in Table 4, in the unit cell of hutchinsonite there are 116 discrete peaks due to  $Pb(Tl)$  vectors, among which  $2 \times 26$  are those due to symmetrical vectors and 64 are the peaks due to cross vectors. These cross vectors have the same weight as those of the screw satellites. By using the above rule among cross vectors, they can be easily distinguished. In Fig. 1, it can be observed that, among possible candidates for the  $c$ -screw satellites,  $D$  and  $E$  have well defined pair peaks  $D'$  and  $E'$  respectively in the section  $z = \frac{1}{4}$ , suggesting that they are the cross vectors. Accordingly, they can be immediately rejected. It is now clear that the peak  $S$  is one of the  $c$ -screw satellites, because it has no pair peak with the same weight in any other sections. The inversion peak  $I$  is then found as indicated in Fig. 1. The peak  $H$  then should be the  $c$ -screw satellite of the other  $(Tl, Pb)$ . However, this peak is multiple with some other peaks, and also in the section  $w = \frac{1}{4}$  there is an elongated multiple peak at the place where the inversion peak



is expected. Therefore, it was not possible to determine the accurate position of the inversion peak in the map. The location of this (Tl, Pb) was found by forming a minimum function based upon the inversion peak *I* of the first (Tl, Pb) in Fig. 4. It was confirmed that the peaks *D* and *E* are the cross-vector peaks of the two sets of (Tl, Pb) atoms. Among them, peak *D* is a cross-vector peak which is called a "conjugate peak" (BUERGER, 1959, pp. 275) (Fig. 5). The final structure revealed that the peak *D* is actually a multiple of  $(\text{Pb, Tl})_{\text{I}} - (\text{Tl, Pb})_{\text{II}}$  and  $(\text{Pb, Tl})_{\text{I}} - \text{As}_{\text{III}}$  cross vectors.

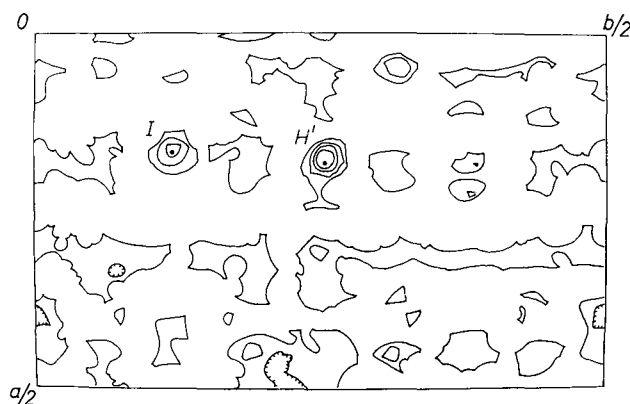


Fig. 4. Minimum function,  $M_2(x, y, \frac{1}{4})$ , based upon the inversion peak, *I*, showing the location of the second Pb(Tl) at *H'*

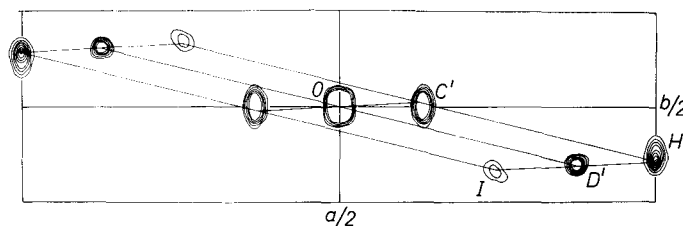


Fig. 5. Inversion peaks of two independent Pb(Tl) atoms and their conjugate peaks *D'* (in the section  $z = \frac{1}{4}$ ) and *C'* (in the section  $z = 0$ )

Based upon the principle given above, an automatic search of inversion peaks may be possible by computing a difference function

$$D(u, v, n) = P(\frac{1}{2} - u, v, \frac{1}{2}) - P(u, v, n)$$

for each section  $n$ . In a favourable case, where serious overlapping of miscellaneous peaks does not occur, the cross-vector peaks, if any,

in the section  $w = \frac{1}{2}$  will become zero in  $D(u, v, n)$  for some section  $n$ , while the  $c$ -screw satellite peaks will not become zero, but show a minimum value corresponding to the weight of the inversion peak for

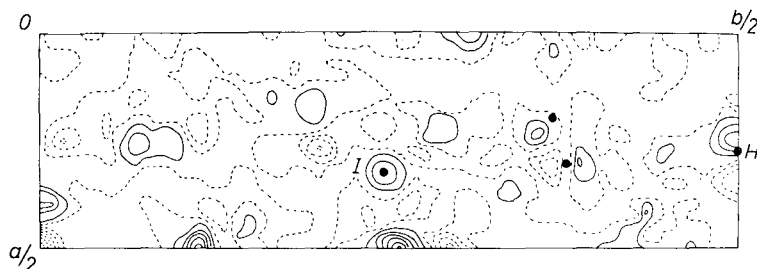


Fig. 6. The difference function  $D(u, v, \frac{1}{4})$ . Possible positions of inversion peaks obtained from the relationship as shown in Fig. 2(b) are indicated by solid circles. The correct inversion peaks  $I$  and  $H'$  are indicated

some section  $n$  where the inversion peak occurs. An example of such a function is given in Fig. 6.

The above method of correctly identifying satellite peaks can readily be applied to any other centrosymmetric space groups which have at least a set of glide planes.

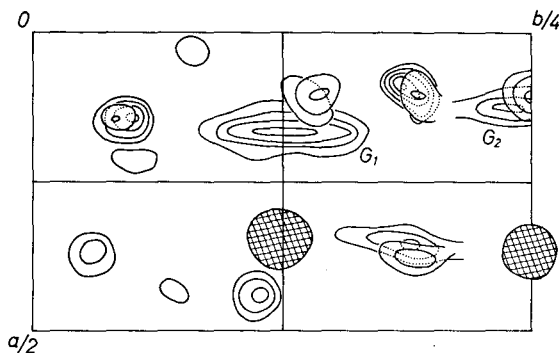


Fig. 7

Fig. 7. Composite diagram of the first three-dimensional Fourier synthesis. Contours for Pb(Tl) atoms are omitted

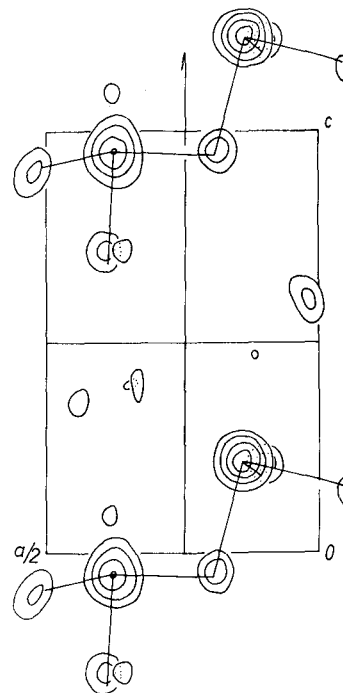


Fig. 8

Fig. 8. Composite diagram of the second three-dimensional Fourier synthesis, showing the range  $y = 0/240$  to  $y = 20/240$  along the  $b$  axis. The final As-S bonds are indicated

*Three-dimensional Fourier series and difference-Fourier trials*

It was not likely that the locations of As and S atoms could be clearly found in the 3D minimum function because the weights of the peaks due to Tl(Pb) — As and Tl(Pb) — S vectors are of the order of the background heights of the Patterson function. Accordingly, a 3D Fourier series was computed based upon the calculated signs from the Tl(Pb) atom locations (Fig. 7). Unfortunately, the coordinates of two Tl(Pb) atoms are close to special positions. Therefore, the signs of the  $F(hkl)$ 's with  $h+l/2 \neq 2n$  and  $l = 2n$ , could not be determined. Because of this restriction, acceptable signs of only about 1200  $F(hkl)$ 's were obtained out of about 2900 reflections. The ill-shaped peaks  $G_1$  and  $G_2$  in Fig. 7 are certainly ghost peaks due to the omission of the above special reflections. In the Fourier map, locations of five As and five S atoms were found with no ambiguity. They were then used to determine the signs for the second 3D Fourier synthesis, in which four further S atoms were found. Part of the composite Fourier map is shown in Fig. 8. For the second synthesis, 1684 acceptable reflections were used. At this stage  $R$  values were found to be 0.199 for  $F(hk0)$  and 0.313 for  $F(0kl)$ . The  $R$  value for  $F(0kl)$  was reduced to 0.225 by a first 2D difference synthesis. Between the two 3D Fourier syntheses, difference synthesis were computed using  $F(hk0)$ 's. Results of these steps of analysis are tabulated in Table 5. The 3D Fourier syntheses were performed at the Computing Center of Oxford University using the program written by O. S. MILLS.

**Least-squares refinement**

The initial stages of the 3D least-squares refinement were performed using the program written by IITAKA for the Bull-Gamma-A.E.T. computer. This program minimizes the function

$$\sum w(hkl) [F_o^2(hkl) - F_c^2(hkl)]^2$$

and uses the diagonal matrix approximation. The weighting scheme chosen was

$$\begin{aligned} w(hkl) &= 1/F^4(hkl) && \text{if } |F_o(hkl)| \geq 4 |F_{o \min}| \\ w(hkl) &= 1/128 F_{o \min}^4 && \text{if } |F_o(hkl)| \leq 4 |F_{o \min}| \\ w(hkl) &= 0 && \text{if } |F_c(hkl)| < F^* \end{aligned}$$

Table 5. Atomic coordinates obtained by various methods

		1	2	3	4	5	6
(Pb,Tl) <sub>I</sub>	<i>x</i>	0.36	0.3648	0.3648	0.3565	0.3580	
	<i>y</i>	0.25	0.2445	0.2445	0.2445	0.2458	0.2458
	<i>z</i>	0.125	0.1234			0.118	0.105
(Tl,Pb) <sub>II</sub>	<i>x</i>	0.336	0.3360	0.3360	0.3360	0.3360	
	<i>y</i>	0.123	0.1250	0.1243	0.1240	0.1229	0.1229
	<i>z</i>	0.625	0.6250			0.630	0.637
As <sub>I</sub>	<i>x</i>		0.104	0.104	0.104	0.107	
	<i>y</i>		0.192	0.192	0.196	0.1937	0.1934
	<i>z</i>		0.70			0.70	0.70
As <sub>II</sub>	<i>x</i>		0.104	0.104	0.104	0.100	
	<i>y</i>		0.192	0.192	0.192	0.1875	0.1875
	<i>z</i>		0.125			0.133	0.133
As <sub>III</sub>	<i>x</i>		0.4376	0.4376	0.4376	0.4374	
	<i>y</i>		0.1112	0.1112	0.1112	0.1145	0.1145
	<i>z</i>		0.1330			0.133	0.142
As <sub>IV</sub>	<i>x</i>		0.146	0.139	0.139	0.144	
	<i>y</i>		0.046	0.0483	0.0483	0.0471	0.0471
	<i>z</i>		0.230			0.220	0.220
As <sub>V</sub>	<i>x</i>		0.375	0.375	0.3742	0.377	
	<i>y</i>		0.0292	0.0292	0.0285	0.0291	0.0291
	<i>z</i>		0.950			0.950	0.950
S <sub>I</sub>	<i>x</i>		0.375	0.385	0.385	0.385	
	<i>y</i>		0.188	0.188	0.188	0.189	0.189
	<i>z</i>		0.375			0.375	0.374
S <sub>II</sub>	<i>x</i>		0.383	0.393	0.400	0.400	
	<i>y</i>		0.188	0.188	0.188	0.1873	0.1872
	<i>z</i>		0.875			0.875	0.875
S <sub>III</sub>	<i>x</i>		0.128	0.128	0.120	0.127	
	<i>y</i>		0.25	0.250	0.250	0.2521	0.2521
	<i>z</i>		0.375			0.368	0.368
S <sub>IV</sub>	<i>x</i>		0.125	0.120	0.120	0.106	
	<i>y</i>		0.140	0.144	0.144	0.1415	0.1415
	<i>z</i>		0.375			0.333	0.333
S <sub>V</sub>	<i>x</i>		0.130	0.124	0.124	0.108	
	<i>y</i>		0.145	0.146	0.146	0.1460	0.1460
	<i>z</i>		0.875			0.90	0.90
S <sub>VI</sub>	<i>x</i>			0.411	0.411	0.411	
	<i>y</i>			0.009	0.009	0.009	0.009
	<i>z</i>					0.685	0.685

Table 5. (Continued)

		1	2	3	4	5	6
S <sub>VII</sub>	<i>x</i>			0.219	0.219	0.200	
	<i>y</i>			0.056	0.056	0.0582	0.0582
	<i>z</i>					0.950	0.950
S <sub>VIII</sub>	<i>x</i>			0.482	0.482	0.44	
	<i>y</i>			0.0868	0.0868	0.083	0.069
	<i>z</i>					0.36	0.37
S <sub>IX</sub>	<i>x</i>			0.0093	0.0093	0.020	
	<i>y</i>			0.0767	0.0767	0.075	0.075
	<i>z</i>					0.60	0.60
<i>R</i>	( <i>hk0</i> )	0.47	0.34	0.271	0.206	0.199	0.181
	( <i>0kl</i> )	0.62				0.313	0.225
	( <i>hkl</i> )						0.295

1. From Patterson diagram.
2. From first 3D Fourier synthesis.
3. From first difference Fourier projection //c.
4. From second difference Fourier projection //c.
5. From second 3D Fourier synthesis.
6. From first difference Fourier projection //a.

Overall temperature factor  $B = 2.0$  was used for structure-factor calculations.

where,  $F_{o\ min}$ , the minimum observable  $F_o$ -value, was taken as 50, and a value of  $F^* = 25$  was used. Three cycles of refinement reduced the initial  $R = 0.295$  as follows:  $0.295 \rightarrow 0.257 \rightarrow 0.224 \rightarrow 0.193$  for all  $F(hkl)$ 's including non-observed ones. This smooth convergence indicates that the structure with the chemical formula  $(Tl, Pb)_2As_5S_9$  is basically correct. Up to this stage, atomic form-factor approximations by VAND *et al.* (1957) were used, but were later changed to the values given by FORSYTH *et al.* (1959). Atoms were assumed to be unionized throughout the refinement, including the successive stages.

Mainly because of the comparatively slow calculating speed of the Bull-Gamma electronic computer, the successive refinement was performed on an IBM 7090 computer using a full-matrix, least-squares program, SFLSQ3, written by C. PREWITT. For the final stages of refinement, form factors based upon the Thomas-Fermi-Dirac statistical method were employed for Pb and Tl, and those given by FREEMAN and WATSON, and DAWSON were used for As and S respectively (International Tables, vol. III, pp. 201 to 212). The weighting scheme

Table 6. *Final atomic parameters of hutchinsonite, and their estimated standard deviations*

	$x$	$y$	$z$	$B$	$\sigma(x) \times 10^{-4}$	$\sigma(y) \times 10^{-4}$	$\sigma(z) \times 10^{-4}$	$\sigma(B) \times 10^{-2}$
(Pb,Tl) <sub>I</sub>	0.3581	0.2469	0.1056	1.92	1.3	0.5	2.1	2.7
(Tl,Pb) <sub>II</sub>	0.3361	0.1223	0.6351	2.85	1.7	0.5	2.4	3.0
As <sub>I</sub>	0.1081	0.1948	0.7040	1.84	3.9	1.1	5.4	7.5
As <sub>II</sub>	0.0994	0.1848	0.1261	2.00	4.0	1.2	5.7	7.1
As <sub>III</sub>	0.4362	0.1153	0.1344	1.86	3.9	1.1	5.5	7.2
As <sub>IV</sub>	0.1364	0.0480	0.2151	1.94	4.0	1.2	5.5	7.2
As <sub>V</sub>	0.3814	0.0288	0.9545	1.91	4.0	1.2	5.6	7.3
S <sub>I</sub>	0.3934	0.1899	0.3644	1.82	9.4	2.8	13.3	17.8
S <sub>II</sub>	0.4090	0.1906	0.8628	1.61	8.9	2.6	12.7	20.4
S <sub>III</sub>	0.1123	0.2540	0.3704	1.46	8.2	2.5	12.7	13.1
S <sub>IV</sub>	0.1289	0.1377	0.3247	1.64	9.0	2.7	12.9	18.7
S <sub>V</sub>	0.1128	0.1466	0.8953	1.55	8.8	2.6	12.7	17.3
S <sub>VI</sub>	0.3878	0.0151	0.6838	2.27	10.3	3.0	14.4	17.4
S <sub>VII</sub>	0.1942	0.0573	0.9521	2.41	10.7	3.1	15.0	18.9
S <sub>VIII</sub>	0.4390	0.0672	0.3275	1.99	9.7	2.9	13.8	20.8
S <sub>IX</sub>	0.0086	0.0799	0.5859	1.70	9.1	2.7	13.0	16.2

recommended by CRUICKSHANK *et al.* (1961) was adopted. This has the form

$$w = 1/(a + F + cF^2).$$

For  $a$  and  $c$ , 90 and 0.002 were used, respectively. Since the  $F_o$ 's were collected around the  $c$  rotation axis from  $l = 0$  to  $l = 7$  and the  $F_o$ 's for each level have different scale factors, the refinement of scale factors was carried out as the first step. In the following steps, refinement of the coordinates and the isotropic temperature factors was performed separately. After four such cycles the  $R$  value went down to 0.145 for all  $F_o$ 's and to 0.123 for the observed reflections alone.

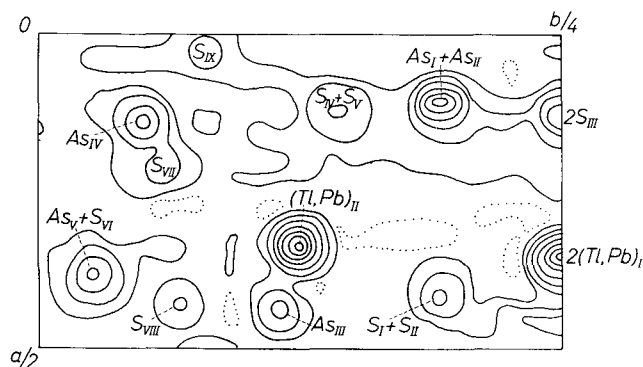


Fig. 9. Final electron-density projection along the  $c$  axis. The contours are drawn at equal, but arbitrary, intervals except for  $\text{Pb(Tl)}_I$  where the interval is doubled: the zero contour is dotted

The final atomic parameters are given in Table 6, with estimated standard deviations. The comparison of  $F_o$ 's and  $F_c$ 's is given in Table 7. The final Fourier projection  $\rho(xy)$  is shown in Fig. 9.

### Discussion of the refinement

The effects of dispersion were not taken into account in the above steps of refinement. With  $\text{CuK}\alpha$  the effect is negligible for As and S, but for Pb (and Tl) it is appreciable,  $\Delta f'$  and  $\Delta f''$  being  $-4$  and  $10 \sim 9$  respectively. Since the isotropic temperature factors of the Pb (Tl) atoms are slightly larger than those of the lighter As and S atoms, and it appeared that this might be due to the neglect of dispersion

Table 7. Comparison of the  $F_o(hkl)$  and the  $\pm F_c(hkl)$  values of hutchinsonite

Table with 16 columns: h k l, Fo, Fc, h k l, Fo, Fc, h k l, Fo, Fc, h k l, Fo, Fc, h k l, Fo, Fc. The table lists numerical values for each parameter across various hkl indices.



Table 7. (Continued)

Table with 15 columns: h k l, F\_o, F\_c, h k l, F\_o, F\_c, h k l, F\_o, F\_c, h k l, F\_o, F\_c, h k l, F\_o, F\_c. It contains a dense grid of numerical data representing crystal structure parameters.



Table 7. (Continued)

Table with 16 columns: k, l, F\_o, F\_c, h, k, l, F\_o, F\_c, h, k, l, F\_o, F\_c, h, k, l, F\_o, F\_c. It contains numerical data for various crystallographic reflections.



Table 8

Results of least-squares refinements using dispersion corrections for Pb and Tl  
 Appreciable differences from the values in Table 6 are observed only for B's of  
 (Tl,Pb)

	<i>x</i>	<i>y</i>	<i>z</i>	<i>B</i>
(Pb,Tl) <sub>I</sub>	0.3581	0.2469	0.1056	1.35
(Tl,Pb) <sub>II</sub>	0.3361	0.1223	0.6350	2.32
As <sub>I</sub>	0.1082	0.1948	0.7040	1.87
As <sub>II</sub>	0.0994	0.1848	0.1261	1.96
As <sub>III</sub>	0.4361	0.1153	0.1343	1.85
As <sub>IV</sub>	0.1365	0.0480	0.2151	1.92
As <sub>V</sub>	0.3814	0.0288	0.9545	1.89
S <sub>I</sub>	0.3933	0.1898	0.3640	1.73
S <sub>II</sub>	0.4092	0.1906	0.8628	1.57
S <sub>III</sub>	0.1123	0.2541	0.3704	1.42
S <sub>IV</sub>	0.1289	0.1377	0.3244	1.67
S <sub>V</sub>	0.1129	0.1466	0.8956	1.58
S <sub>VI</sub>	0.3877	0.0150	0.6839	2.31
S <sub>VII</sub>	0.1942	0.0573	0.9521	2.36
S <sub>VIII</sub>	0.4390	0.0671	0.3276	2.03
S <sub>IX</sub>	0.0087	0.0800	0.5856	1.70

### Description of the structure

The interatomic distances and bond angles are tabulated in Table 9 and Table 10. A diagrammatic representation of the structure is given in Fig. 10, from which it can be observed that the structure consists of two kinds of slabs, *A* and *B*, parallel to (010). The *A* slabs

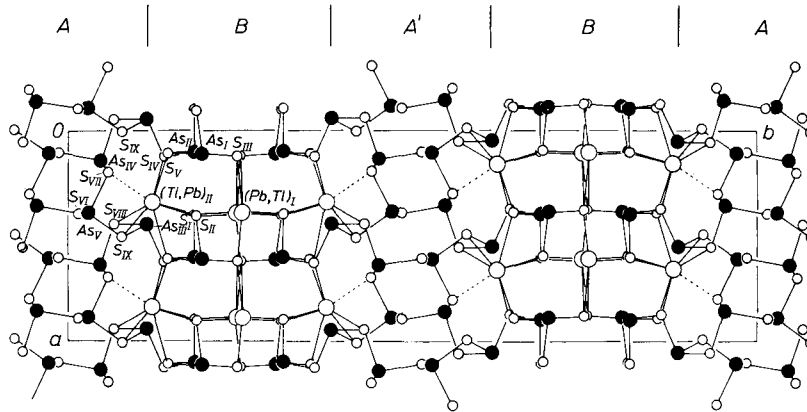


Fig. 10. The *c*-axis projection of the structure of hutchinsonite. Large open circle: Pb (Tl), solid circle: As, and small open circle: S. The slabs *A'* and *B'* are related respectively to *A* and *B* by the *b*-glide or *b*-screw operations

Table 9. (Tl, Pb)—S and As—S distances in hutchinsonite

	S <sub>I</sub>	S <sub>II</sub>	S <sub>III</sub>	S <sub>IV</sub>	S <sub>V</sub>	S <sub>VI</sub>	S <sub>VII</sub>	S <sub>VIII</sub>	S <sub>IX</sub>	mean	$\sigma(l)$
Pb(Tl) <sub>I</sub>	2.94 Å 3.00	2.86 Å 3.10	2.77 Å 3.43 3.28							3.05 Å	± 0.01 <sub>0</sub>
Tl(Pb) <sub>II</sub>	3.31	3.15		3.43 Å	3.33 Å 3.12		(3.79) Å	3.37 Å	3.30 Å	3.29*	
As <sub>I</sub>		2.30	2.26		2.31					2.29	± 0.01 <sub>1</sub>
As <sub>II</sub>	2.24			2.35	2.32					2.30	
As <sub>III</sub>				2.25				2.32	2.33	2.30	
As <sub>IV</sub>						2.26	2.26	2.27		2.26	
As <sub>V</sub>						2.26	2.27		2.29	2.27	

\* Excluding Pb(Tl)<sub>II</sub>—S<sub>VII</sub> distance.

Table 10  
Bond angles and *S-S* edge lengths of *As-S* pyramids in hutchinsonite

As <sub>I</sub> pyramid			
S <sub>III</sub> -S <sub>V</sub>	3.52 Å	S <sub>III</sub> -As-S <sub>V</sub>	105.9°
S <sub>III</sub> -S <sub>II</sub>	3.66	S <sub>III</sub> -As-S <sub>II</sub>	106.3
S <sub>V</sub> -S <sub>II</sub>	3.59	S <sub>V</sub> -As-S <sub>II</sub>	102.1
mean	3.59		104.8
As <sub>II</sub> pyramid			
S <sub>IV</sub> -S <sub>V</sub>	3.52	S <sub>IV</sub> -As-S <sub>V</sub>	97.9
S <sub>IV</sub> -S <sub>I</sub>	3.50	S <sub>IV</sub> -As-S <sub>I</sub>	99.7
S <sub>V</sub> -S <sub>I</sub>	3.44	S <sub>V</sub> -As-S <sub>I</sub>	97.9
mean	3.49		98.5
As <sub>III</sub> pyramid			
S <sub>VIII</sub> -S <sub>IX</sub>	3.49	S <sub>VIII</sub> -As-S <sub>IX</sub>	97.2
S <sub>VIII</sub> -S <sub>IV</sub>	3.46	S <sub>VIII</sub> -As-S <sub>IV</sub>	98.2
S <sub>IX</sub> -S <sub>IV</sub>	3.23	S <sub>IX</sub> -As-S <sub>IV</sub>	89.6
mean	3.39		95.0
As <sub>IV</sub> pyramid			
S <sub>VII</sub> -S <sub>VI</sub>	3.30	S <sub>VII</sub> -As-S <sub>VI</sub>	93.9
S <sub>VII</sub> -S <sub>VIII</sub>	3.31	S <sub>VII</sub> -As-S <sub>VIII</sub>	94.1
S <sub>VI</sub> -S <sub>VIII</sub>	3.46	S <sub>VI</sub> -As-S <sub>VIII</sub>	99.7
mean	3.36		95.9
As <sub>V</sub> pyramid			
S <sub>VI</sub> -S <sub>VII</sub>	3.38	S <sub>VI</sub> -As-S <sub>VII</sub>	96.6
S <sub>VI</sub> -S <sub>IX</sub>	3.24	S <sub>VI</sub> -As-S <sub>IX</sub>	90.6
S <sub>VII</sub> -S <sub>IX</sub>	3.50	S <sub>VII</sub> -As-S <sub>IX</sub>	100.6
mean	3.37		95.9
$\sigma(l) = \pm$	0.01 <sub>4</sub> Å	$\sigma(\theta) = \pm$	0.5°

are composed of infinite spiral chains of As-S pyramids around the two-fold screw axes. These chains are extended along the *c* axis, a configuration which is somewhat similar to that found in lorandite TlAsS<sub>2</sub> (ZEMANN and ZEMANN, 1959). The chains in hutchinsonite are, however, laterally bonded together by additional AsS<sub>3</sub> pyramids to form a complex layer parallel to (010), Fig. 11. The bond lengths and angles of these spiral chains are shown in Fig. 12.

The *B* slabs are composed of Pb(Tl), As and S, and the structure of these slabs is somewhat similar to a distorted PbS-type structure. Accordingly, the As atoms in the *B* slabs (As<sub>I</sub>, As<sub>II</sub>) have six neighbouring sulfur atoms at distances As<sub>I</sub>: 2.30, 2.26, 2.31, 3.43, 3.50, 3.83 Å; As<sub>II</sub>: 2.24, 2.32, 2.35, 3.16, 3.22, 3.72 Å. If account is taken of the nearest neighbours only, each As atom has a pyramidal coordination of three sulfurs, just as in an *A* slab. These As-S groups form

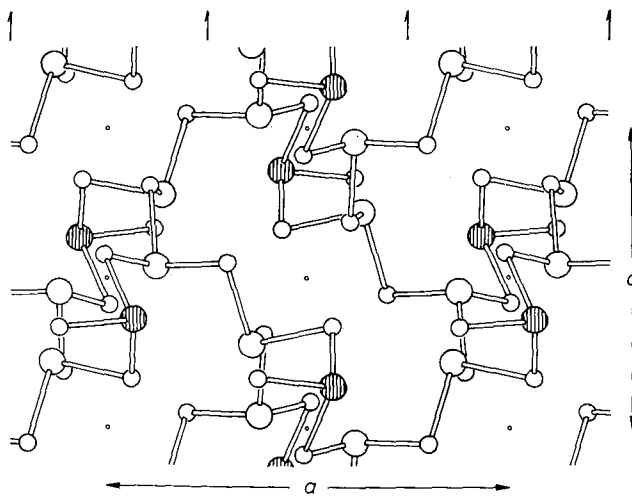


Fig. 11. The  $b$ -axis projection of the slab A. Large circle: As, small circle: S. The shaded large circle indicates  $As_{III}$ . The  $c$ -screw axis and center of symmetry are shown

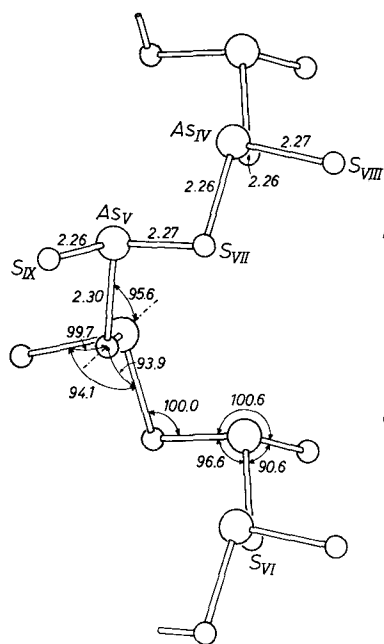


Fig. 12

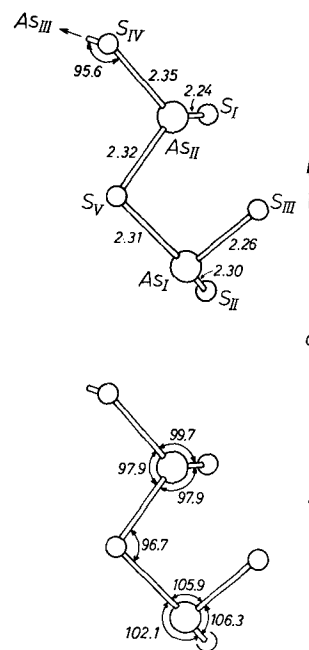


Fig. 13

Fig. 12. As-S spiral chain, as viewed along the  $b$  axis

Fig. 13.  $As_2S_5$  groups in the slab B, as viewed along the  $a$  axis



a finite group  $\text{As}_2\text{S}_5$  which is shown in Fig. 13. The *A* and *B* slabs are joined together by  $(\text{Tl,Pb})_{\text{II}}$  and  $\text{As}_{\text{III}}$  atoms, and thus they build up the bulk of the structure. This nature of the structure explains well the good cleavage parallel to (010). The configuration of the  $\text{As}_{\text{III}}\text{-S}$  group is given in Fig. 14.

The unit cell contains 72 S, 40 As and 16 (Tl, Pb) atoms, giving the chemical formula  $(\text{Tl,Pb})_2\text{As}_5\text{S}_9$ . In Table 2, it is observed that, for  $d = 4.6$ , the total number of Ag + As is close to 40 for the analyses

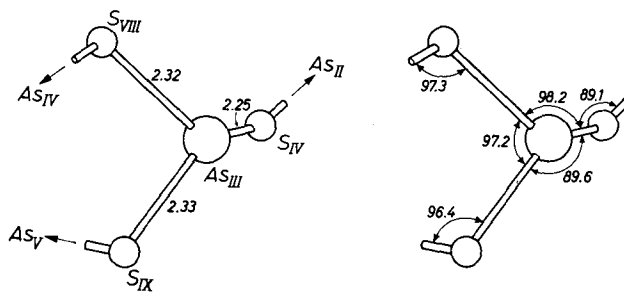


Fig. 14.  $\text{As}_{\text{III}}\text{-S}$  pyramids, as viewed along the *a* axis.

1, 2 and 3. This fact suggests that Ag may replace some sites of As. Though such an example has not been reported, it is conceivable because examples have been reported where Ag has trigonal pyramidal coordination.

In miargyrite,  $\text{AgSbS}_2$  (KNOWLES, 1964) and smithite,  $\text{AgAsS}_2$  (HELLNER and BURZLAFF, 1964), Ag has six neighbours of S atoms, of which the three nearest form a pyramidal coordination as for As in  $\text{AsS}_3$ . An attempt was made to prove the above hypothesis by examining Wiesloch hutchinsonite which is reported to be rich in Ag, though a complete chemical analysis is not given (SEELIGER, 1954). The intensity distribution of the (*hk*0) reflections does not show any differences from that of the Binnatal specimens which we used. A calculation showed that even if there are 8 Ag atoms in the unit cell and they are distributed over the 40 As sites, the electron number for each site will be increased to 34.4, which is higher only by 1.4 than that of As. If this is the case, it is hardly possible to detect the difference.

It should be noted that the As-S bond lengths in the  $\text{As}_4\text{S}_8$  spiral chains are nearly equal, and they give a mean value  $2.27 \pm 0.01$  Å, which shows good agreement with the value  $2.28 \pm 0.007$  Å for the  $\text{As}_{\text{III}}\text{-S}$  single-bond length (CAMERMAN and TROTTER, 1964). On the other hand, each of the  $\text{As}_{\text{III}}\text{-S}$ ,  $\text{As}_{\text{II}}\text{-S}$  and  $\text{As}_{\text{I}}\text{-S}$  pyramids is characteri-

zed by having one short As—S bond length of about 2.25 Å and two longer ones of around 2.32 Å. The contents of Cu as shown in the chemical analyses 2 and 3 in Table 1, are not essential to the structure. A discussion of the possible locations of this atom is beyond the scope of the present investigation.

The chemical analyses show that there are about the same numbers of Pb and Tl atoms in the unit cell. Calculation of interatomic distances shows that the mean (Tl,Pb)<sub>II</sub>—S distance is bigger than the (Pb,Tl)<sub>I</sub>—S distance, and also the temperature factor of the former is somewhat higher than that of the latter. The configuration of seven sulfur atoms coordinated to a (Pb,Tl)<sub>I</sub> atom is similar to the configuration of Pb in other sulfosalts, while the irregular configuration for (Tl,Pb)<sub>II</sub> (coordination number = 7 + 1) is uncommon for Pb. An irregular configuration of sulfur atoms around Tl has been reported in lorandite (ZEMANN and ZEMANN, 1959). This fact may suggest that the (Pb,Tl)<sub>I</sub> site is mainly occupied by Pb and the (Tl,Pb)<sub>II</sub> site by Tl. Since, for the structure-factor calculation, the mean of the form factors of these atoms was used, a possible ordering of these atoms was tested using  $F(hk0)$  data. If we assume complete ordering by placing Pb at the (Pb,Tl)<sub>I</sub> site and Tl at the (Tl,Pb)<sub>II</sub> site, the  $R$  value for the  $F(hk0)$  data improves by 0.4%. If we use  $f_{\text{Pb}}$  for both sites, the temperature factor of (Pb,Tl)<sub>I</sub> decreases by only 0.01, while that of (Tl,Pb)<sub>II</sub> increases by 0.2. Although the changes are very small and may not be significant, they are consistent with the assumption that (Pb,Tl)<sub>I</sub> sites are mainly occupied by Pb and (Tl,Pb)<sub>II</sub> by Tl.

In the  $B$  slabs, each Pb(Tl) atom and its neighbouring S atom build up a chain along the  $c$  axis. These chains are joined laterally by sharing a S atom to form the framework of  $B$  slabs. This kind of linkage of Pb—S is common to most of the sulfosalts which have so far been investigated (IITAKA and NOWACKI, 1962; LEINWEBER, 1956; NIIZEKI and BUERGER, 1957; NOWACKI *et al.*, 1961, 1963a; WEITZ and HELLNER, 1960).

The Pb—S chains have a periodicity of around 4 Å. The S—S distances in the SbS<sub>3</sub> pyramids are close to 4 Å. Therefore, in the sulfosalts containing Pb and Sb, SbS<sub>3</sub> pyramids may form a chain or a group which fits to the 4 Å period of the Pb—S chain. On the other hand, the S—S distances of the AsS<sub>3</sub> pyramids are around 3.5 Å. Accordingly, the AsS<sub>3</sub> pyramids do not fit to the Pb—S chain, and they tend to form a complex group, causing the complexity of the structure. It was reported by LEBIHAN (1962) that the  $x\text{PbS} \cdot y\text{As}_2\text{S}_3$  sulfosalts of the

second group mentioned in the introduction have infinite  $\text{AsS}_2$  chains along the Pb-S chains. However, refined structures (NOWACKI *et al.*, 1963a) have proved that every four  $\text{AsS}_3$  pyramids form a complex finite group in these structures. This fact explains why the short axis (4 Å) does not occur in the sulfosalts containing As, as compared to those containing Sb. It is interesting to note that the above situation observed in sulfosalts is somewhat similar to the structures of silicates where a misfit between octahedral and tetrahedral configurations causes complexity of the structure (TAKÉUCHI, 1964).

*Acknowledgements.* — We thank Dr. H. BÜRKI and cand. phil. V. KUNZ for various help and Dr. N. D. JONES for having improved the English of this paper; Dr. J. S. ROLLETT (Oxford University Computing Laboratory), Prof. W. NEF and Dr. R. HÜSSER (Rechenzentrum der Universität und der Finanzdirektion des Kantons Bern), Dr. C. A. HÉRITIER (I.B.M. Geneva) for many invaluable calculations. The IBM Corporation kindly put at our disposal its 7090 machine at CERN, Geneva. Hutchinsonite crystals were kindly provided by Dr. H. ADRIAN (Naturhistorisches Museum Bern), Prof. E. SEELIGER (Berlin) and the Mineralogisches Institut in Heidelberg. Dr. ST. GRAE-SER kindly made a spectrochemical analysis. The investigation was generously supported by Schweizerischer Nationalfonds and Kommission zur Förderung der wissenschaftlichen Forschung and by the Stiftung Entwicklungsfonds Seltene Metalle.

#### References

- M. J. BUEGER (1959), Vector space and its application in crystal-structure investigation. John Wiley and Sons, New York.
- N. CAMERMAN and J. TROTTER (1964), Stereochemistry of arsenic. Part XI. "Cacodyl disulphide", dimethylarsino dimethyldithioarsinate. *J. Chem. Soc. [London]* 219–227.
- D. W. J. CRUICKSHANK, D. E. PILLING, A. BUJOSA, F. M. LOVELL and M. R. TRUTER (1961), Crystallographic calculations on the Ferranti Pegasus and Mark I computers. In: Computing methods and the phase problem in x-ray crystal analysis. Pergamon Press, London, pp. 32–78.
- J. B. FORSYTH and M. WELLS (1959), On an analytical approximation to the atomic scattering factor. *Acta Crystallogr.* **12**, 412–415.
- E. HELLNER und H. BURZLAFF (1964), Die Struktur des Smithits  $\text{AgAsS}_2$ . *Naturwissenschaften* **51**, 35–36.
- International tables for x-ray crystallography, vol. III. (1962), Kynoch Press, Birmingham.
- Y. IITAKA and W. NOWACKI (1962), A redetermination of the crystal structure of galenobismutite,  $\text{PbBi}_2\text{S}_4$ . *Acta Crystallogr.* **15**, 691–698.

- CH. R. KNOWLES (1964), A redetermination of the structure of miargyrite,  $\text{AgSb}_2$ . *Acta Crystallogr.* **17**, 847–851.
- M.-TH. LEBIHAN (1962), Étude structurale de quelques sulfures de plomb et d'arsenic naturels du gisement de Binn. *Bull. Soc. franç. Min. Cristallogr.* **85**, 15–47.
- G. LEINWEBER (1956), Struktur-Analyse des Bournonits und Seligmannits mit Hilfe der Superpositions-Methoden. *Z. Kristallogr.* **108**, 161–184.
- N. NIIZEKI and M. J. BUERGER (1957), The crystal structure of jamesonite,  $\text{FePb}_4\text{Sb}_6\text{S}_{14}$ . *Z. Kristallogr.* **109**, 161–183.
- W. NOWACKI (1964), Zur Kristallchemie der Sulfosalze, insbesondere aus dem Lengenbach (Binnatal, Kt. Wallis). *Schweiz. Min. Petr. Mitt.* **44**, 459–484, espec. Table 2.
- W. NOWACKI, H. BÜRKI, Y. ITAKA and V. KUNZ (1961), Structural investigations on sulfosalts from the Lengenbach, Binn Valley (Ct. Wallis). Part 2. *Schweiz. Min. Petr. Mitt.* **41**, 103–116.
- W. NOWACKI, C. BAHEZRE and F. MARUMO (1963a), Investigations on sulphosalts from Binnatal (Ct. Wallis, Switzerland). *Acta Crystallogr.* **16**, A 11–12.
- W. NOWACKI und C. BAHEZRE (1963b), Die Bestimmung der chemischen Zusammensetzung einiger Sulfosalze aus dem Lengenbach (Binnatal, Kt. Wallis) mit Hilfe der elektronischen Mikrosonde. *Schweiz. Min. Petr. Mitt.* **43**, 407–411.
- W. NOWACKI, F. MARUMO und Y. TAKÉUCHI (1964), Untersuchungen an Sulfiden aus dem Binnatal (Kt. Wallis, Schweiz). *Schweiz. Min. Petr. Mitt.* **44**, 5–9.
- E. W. NUFFIELD (1947), X-ray measurements on hutchinsonite. *Univ. Toronto Studies, Geol. Ser. No.* **51**, 79–81.
- H. RÖSCH (1963), Zur Kristallstruktur des Grattonits —  $9 \text{PbS} \cdot 2 \text{As}_2\text{S}_3 \cdot \text{N}$ . *Jb. Min. Abh.* **99**, 307–337.
- E. SEELIGER (1954), Ein neues Vorkommen von Hutchinsonit in Wiesloch in Baden. *N. Jb. Min. Abh.* **86**, 163–178.
- G. E. SMITH and G. T. PRIOR (1907), Red silver minerals from the Binnenthal, Switzerland. *Min. Mag.* **14**, 283–307.
- H. E. SWANSON and E. TATGE (1953), Standard x-ray diffraction powder patterns. *NBS. Circular* **539**, I 66–67.
- Y. TAKÉUCHI (1964), Structures of brittle micas. To appear in the *Proc. of the Madison Clay Conference*.
- Y. TAKÉUCHI, S. GHOSE and W. NOWACKI (1964), The crystal structure of the thallium-lead sulfosalt hutchinsonite. *Chimia* **18**, 215–217.
- V. VAND, P. E. ELLAND and R. PEPINSKY (1957), Analytical representation of atomic scattering factors. *Acta Crystallogr.* **10**, 303–306.
- G. WEITZ und E. HELLNER (1960), Über komplex zusammengesetzte sulfidische Erze. VII. Zur Kristallstruktur des Cosalits,  $\text{Pb}_2\text{Bi}_2\text{S}_5$ . *Z. Kristallogr.* **113**, 385–402.
- A. ZEMANN und J. ZEMANN (1959), Zur Kenntnis der Kristallstruktur von Lorandit,  $\text{TlAsS}_2$ . *Acta Crystallogr.* **12**, 1002–1006.